

Characterization of the temporal accumulation of minute virus of mice replicative intermediates

Greg Tullis,[†] Robert V. Schoborg[‡] and D. J. Pintel*

Molecular Microbiology and Immunology, University of Missouri, School of Medicine, Columbia, Missouri 65212, U.S.A.

We have characterized the temporal appearance and accumulation of minute virus of mice (MVM) replicative forms (RF) in highly synchronized single rounds of infection using a combination of restriction endonuclease analysis and two-dimensional agarose gel electrophoresis. Between 4 and 12 h after release of infected cells into the S-phase, both monomer (mRF) and dimer RF (dRF) increased exponentially at similar rates such that the ratio of mRF relative to dRF remained unchanged. These DNA forms accumulated at a faster rate than MVM RNAs, suggesting that the number of DNA templates available for replication is limiting, not the expression of MVM gene products, and that the majority of DNA templates are likely to be destined for DNA amplification rather than transcription and further gene expression. During this exponential DNA amplification phase, approximately 65% of mRF were in a fully extended form, whereas most of the remaining mRF were covalently closed in the left end and extended in the right end. Although MVM replication presumably generates right-hand turn-around

mRF, only a low level of this form persists (5 to 10% of total mRF) at all times examined, suggesting that this form must be quickly converted to the extended form. Greater than 90% of dRF, which have right-hand palindromes on both ends of the molecule, were extended on both ends. A significant proportion of dRF and higher concatemers are nicked in the left-hand palindrome, suggesting that resolution of dRF into two mRFs may occur via single-stranded nicks rather than a double-stranded cut. An additional replicative form, previously termed band X, has been identified as an RNA–DNA duplex. This band is formed predominantly intracellularly, before cell lysis but its biological significance remains unclear. Our results provide direct experimental support for many of the predictions of the current models of parvovirus replication and suggest that the kinetic hairpin transfer model should be adjusted to include a strand-transfer or similar mechanism for the resolution of dRF to account adequately for the production of left-end turn-around forms.

Introduction

Minute virus of mice (MVM) is among the best characterized of the parvoviruses, which are unique among viruses of vertebrates in that they package a linear, single-stranded DNA molecule. Parvoviruses replicate in the nucleus of infected cells via linear, double-stranded, episomal DNA molecules utilizing a hairpin transfer mechanism to replicate the ends of their linear DNA molecule (Cavalier-Smith, 1974; Straus *et al.*, 1976; Tattersall & Ward, 1976). Terminal palin-

dromes prime viral DNA replication by folding back upon themselves to form a hairpin structure. Subsequent extension from the 3' terminus generates a linear, double-stranded DNA molecule that is covalently closed at one end. This covalently closed (or turn-around) form can then be converted back to an open (or extended) end by the introduction of a strand-specific nick directly adjacent to the terminal palindrome followed by extension toward the end of the molecule by a cellular DNA polymerase.

Adeno-associated virus (AAV), another parvovirus, has identical palindromes of 125 nucleotides (nt) on both ends of the genome which can fold into T-shaped structures. Replication of the AAV genome can initiate at either end of the DNA to generate approximately equal amounts of both orientations (called flip and flop) in both ends, and the orientation of one end is independent of the other (Lusby *et al.*, 1981). MVM, on

* Present address: Department of Molecular Biology, Princeton University, Princeton, New Jersey, U.S.A.

† Present address: Division of Comparative Medicine, Johns Hopkins School of Medicine, Baltimore, Maryland, U.S.A.

the other hand, has two very different structures on the left and right ends. The left (or 3') palindrome is 115 nt long and can fold into a T-shaped hairpin similar to AAV termini (Astell *et al.*, 1983). The right (or 5') palindrome is 206 nt long and contains small, internal inverted repeats, which may form a small cruciform structure (Astell *et al.*, 1983; Merchlinsky, 1984). Like that of AAV, the right hairpin of MVM is found in two orientations. The left hairpin, however, although structurally more similar to AAV termini than the right palindrome, is found exclusively in one orientation (arbitrarily designated as flip), suggesting that the left hairpin of MVM is not resolved by a hairpin transfer mechanism (Astell *et al.*, 1983, 1985). Because the incoming single-stranded (ss) DNA is presumably converted to monomer replicative forms (mRF) by extension from the left (3') hairpin to produce an mRF covalently closed in the left end (depicted in Fig. 3c, ix), MVM DNA is predicted to pass through an obligatory dimeric replicative form (dRF). During AAV infection dRF are also seen but they are presumably not obligatory, because both termini can be converted to the extended form.

Astell and co-workers (1983, 1985) have proposed a role for the terminal protein (NS1) in the resolution of dRF into two mRF. They suggested that NS1 may have a nicking and strand transfer activity similar to the ϕ X174 gene A protein and topoisomerase I in the dimer bridge region and become covalently attached to the 5' phosphate. Replication would then initiate at the newly exposed 3' OH and progress across the dimer bridge to the opposition NS1 cleavage site, at which point NS1 would cleave the opposite strand, catalyse the ligation of the 5' end of the original strand to the 3' end of the opposite site and become covalently attached to the new 5' end. As predicted by this model, cloned dimer bridge fragments are resolved into both turn-around and extended ends by NS1 (Cotmore & Tattersall, 1992; Cotmore *et al.*, 1992). However, recent analysis of nicked but unresolved dimer bridge fragments suggests that the initial nick may occur on the strand opposite to that predicted by the original model (Cotmore *et al.*, 1993).

Although the modified rolling hairpin model of Astell *et al.* (1983, 1985) provides a satisfactory explanation for MVM DNA forms, it does not adequately account for DNA forms observed in the replication of other parvoviruses. For example, LuIII has two non-identical left and right hairpins very similar to those of MVM, but unlike MVM, LuIII packages approximately equivalent amounts of plus and minus strands (Muller & Siegl, 1983; Bates *et al.*, 1984). Of the packaged ssDNA, minus strands are found exclusively in the flip orientation in the left end and both orientations in the right end, similar to the situation for MVM. Plus strands, however, are found in both orientations in both ends. Therefore, if minus

strands of LuIII are exclusively flip in the left end because of an inherent inability to initiate replication from the left hairpin, as proposed for MVM, then plus strands must be generated by a different mechanism.

Recently, a unifying model for parvoviral DNA replication, called the kinetic hairpin transfer model, has been proposed (Chen *et al.*, 1989; Tyson *et al.*, 1990). This model is based on the simple assumption that different hairpin conformations (flip or flop) may be processed at different rates and successfully accounts for the accumulation of the different DNA conformations observed with AAV, MVM, LuIII and bovine parvovirus. For AAV, which has identical palindromes on both ends, both conformations would presumably be processed at equivalent rates. This would generate equivalent amounts of flip and flop orientations in both ends and produce equivalent amounts of plus and minus progeny ssDNA. For MVM, the rate of transfer of the left hairpin would approach zero for the flip conformation, but not for the flop orientation as assumed in the modified rolling hairpin model.

Both the modified rolling hairpin and kinetic hairpin models require discrimination between flip and flop orientations in the left palindrome of MVM. The modified rolling hairpin model predicts that this discrimination occurs during the resolution of the dimer, whereas the kinetic hairpin model predicts that discrimination occurs during the hairpin transfer step. dRF can be resolved by a number of mechanisms including a staggered double-stranded cut. In either case, the discrimination between flip and flop orientations in the left palindrome of MVM must be limited to mismatches (seven/115 nt) within the palindrome, suggesting that NS1 may recognize one of these sites.

In this study we have quantified the temporal accumulation of MVM RF in a single round of a highly synchronized, low multiplicity infection using a combination of restriction enzyme analysis and one- and two-dimensional agarose gel electrophoresis (1D-AGE and 2D-AGE, respectively). 2D-AGE separates intracellular MVM DNA into a pattern consistent with the electrophoretic behaviour expected of putative parvoviral replicative intermediates. Our results indicate that MVM RF are predominantly in the extended conformation on both ends during early times after release of infected cells into the S-phase (0 to 12 h) and that the majority of turn-around mRF at early times in infection are covalently closed in the left end and extended in the right end. MVM mRF covalently closed in the right hairpin are also present and are probably derived from transient replicative intermediates. Our results directly confirm many of the predictions of the current models of parvovirus replication; however, we also suggest that the kinetic hairpin model should be modified to include a

strand-transfer, or similar mechanism, for the resolution of dRF, in order to account for the production of left end turn-around forms.

Methods

Cells and virus. A9_{2L} cells were synchronized by a combination of isoleucine deprivation for 46 h and treatment with aphidicolin for 20 h as described previously (Cotmore & Tattersall, 1987; Clemens & Pintel, 1988). Cells were infected at the time of the aphidicolin block with MVM_p (0.2 p.f.u. per cell) prepared from infected A9_{2L} cells in 50 mM-Tris-HCl pH 8.7, 1 mM-EDTA as previously described (Tattersall & Bratton, 1983). At various times after release from the aphidicolin block, cells from duplicate plates were rinsed three times in PBS and lysed (in 2% SDS, 0.15 M-NaCl, 10 mM-Tris-HCl pH 7.5 and 1 mM-EDTA) and the cellular DNA was sheared as previously described (Tullis *et al.*, 1992). Murine A9_{2L} cells were also pre-labelled with [³H]thymidine (1 µCi/ml) for 24 h as previously described (Tullis *et al.*, 1992), so that viral RF could be standardized to an equivalent number of cells. Each sample was assayed in triplicate for incorporated ³H using DE81 filters (Maniatis *et al.*, 1982) and compared to incorporated ³H determined from a known number of uninfected cells isolated prior to release from the aphidicolin block and that were processed in parallel.

Analysis of MVM DNA and RNA. Viral DNA was visualized by probing Southern blots with a ³²P-labelled, MVM-specific probe generated using random primers (Pharmacia; Feinberg & Vogelstein, 1983) or strand-specific RNA probes generated from the MVM HaeIII C fragment (nt 1854 to 2378) as described (Clemens & Pintel, 1988). ³²P-labelled ssDNA was prepared from DNA extracted from virions by extending the 3' end with radiolabelled dATP, in the presence of ddGTP, ddTTP and ddCTP, using the Klenow fragment of DNA polymerase I (specific activities ranged from 2 × 10⁶ to 5 × 10⁶ c.p.m./µg). Alkaline agarose gels were prepared as previously described (Ogden & Adams, 1987). In order to digest MVM DNA with *Bst*EII and *Bgl*I, MVM DNA was isolated from crude SDS lysates by a modification of the method of Hirt (1967). Briefly, SDS lysates were first treated with proteinase K (0.5 mg per ml at 37 °C for 4 h). NaCl was then added to a final concentration of 1 M and the SDS was allowed to precipitate on ice overnight. The SDS was removed by centrifugation (40000 r.p.m. in a Beckman TLA-45 rotor for 40 min) and the resulting supernatant was treated with RNase A (0.1 mg per ml at 37 °C for 1 h) before extraction with phenol and chloroform:isoamyl alcohol (24:1) and precipitation in ethanol. RNase protection assays were performed exactly as described by Schoborg & Pintel (1991), using an RNA probe generated as above.

Quantification of MVM RF. The number of mRF present in each sample was measured by quantifying the amount of ³²P-labelled probe bound to mRF on Southern blots relative to that bound to MVM plasmid DNA of a known concentration, using a Molecular Dynamics Phosphoimager. This method allowed the detection of less than one mRF copy per cell (data not shown). The amount of MVM ssDNA present per cell was calculated similarly after multiplying the amount of ³²P bound to MVM sDNA by two to compensate for the number of DNA strands present in each molecule. Likewise, the number of dRF (10.2 kb) present per mRF (5.15 kb) was calculated by dividing the amount of ³²P-label bound to dRF by 1.98 to adjust for the difference in size between the two molecules. The amount of mRF that was covalently closed in one or both ends (mT and mC, respectively) was defined as the mRF that migrated at 10 kb in alkaline agarose gels (as shown in Fig. 2d) or, alternatively, as the amount of mRF that was resistant to heat denaturation and quick cooling on ice. Both methods

gave essentially the same result in all three experiments. Therefore, assuming mRF = mE + mL + mR + mC (where mE represents mRF that are extended on both ends, and mL and mR represent mRF that are covalently closed in the left or right ends, respectively) and mT = mL + mR, mE = mRF - (mT + mC). The amount of mC at 12 h following release into the S-phase was quantified from Southern blots of 2D-AGE gels (see Fig. 2d).

The number of mL and mR were calculated from the amount of left (L_e) and right (R_e) turn-around end fragments following digestion with *Bst*EII and *Bgl*I (or *Bgl*I alone). Turn-around and extended restriction fragments were separated by 1D-AGE either directly or following denaturation at 100 °C for 5 min and chilling on ice, which more effectively separates turn-around end fragments from their extended counterparts (L_e and R_e).

Because dRF do not contribute to the left end restriction fragments observed (see Fig. 5, bottom), we can assume (1) $L_e = mE + mR$ and (2) $L_t = mL + mC$. And, because $mL \gg mC$ for all time points examined, (3) $mL \leq L_t$. However, dRF do contribute to the pool of right-end fragments, therefore (4) $R_e = 2dE + dT + mE + mL$ and (5) $R_t = 2dC + dT + mR + mC$, where dE represents dRF that are extended on both ends, dT are dRF that are covalently closed at one end, and dC are dRF that are covalently closed at both ends. Because mC , dT and dC are very small in comparison to mR , mR can be estimated as (6) $mR \leq R_t$ (at 12 h post-release $mR \leq R_t - mC$).

Since $mT = mL + mR$, a lower limit for mL and mR can be estimated from R_t and L_t , respectively, as follows: (7) $mL \geq mT - R_t$ and (8) $mR \geq mT - L_t$. Similarly, fully extended mRF (mE) can be calculated from restriction enzyme digests as (9) $mE = L_e - R_t$.

Results and Discussion

Analysis of the temporal accumulation of MVM RF in highly synchronous infection by 1D-AGE

Following infection of murine A9_{2L} cells at an m.o.i. of 0.2, approximately 90 input MVM ssDNA molecules remained associated per cell at the time of the release of cells into the S-phase (Fig. 1a, 0 h; Table 1). Therefore, only 0.2% of the virions bound progress to productive infection. Viral mRF synthesis was first detected 3 to 4 h after release of cells into the S-phase (at approximately two copies/cell) using 1D-AGE, and dRF was detected (at approximately one copy/cell) 5 to 6 h post-release (Fig. 1a; Table 1). Although the persistence of input ssDNA prohibited the precise analysis of progeny ssDNA early in the infection, an increase in ssDNA, over the residual input, was detected by 8 h into the S-phase, consistent with previous observations that progeny ssDNA is produced as early as 6 h into the S-phase (Cotmore & Tattersall, 1987). All viral DNA forms increase exponentially between 6 and 12 h post-release, and the ratio of dRF to mRF remained similar throughout infection (Table 1). The ratio of accumulated ssDNA relative to double-stranded RF, however, increased between 8 and 12 h post-release (during which time the great majority of ssDNA present was generated during infection) in two experiments, suggesting that MVM had entered a packaging phase by this point during these infections (Table 1). Because we have only

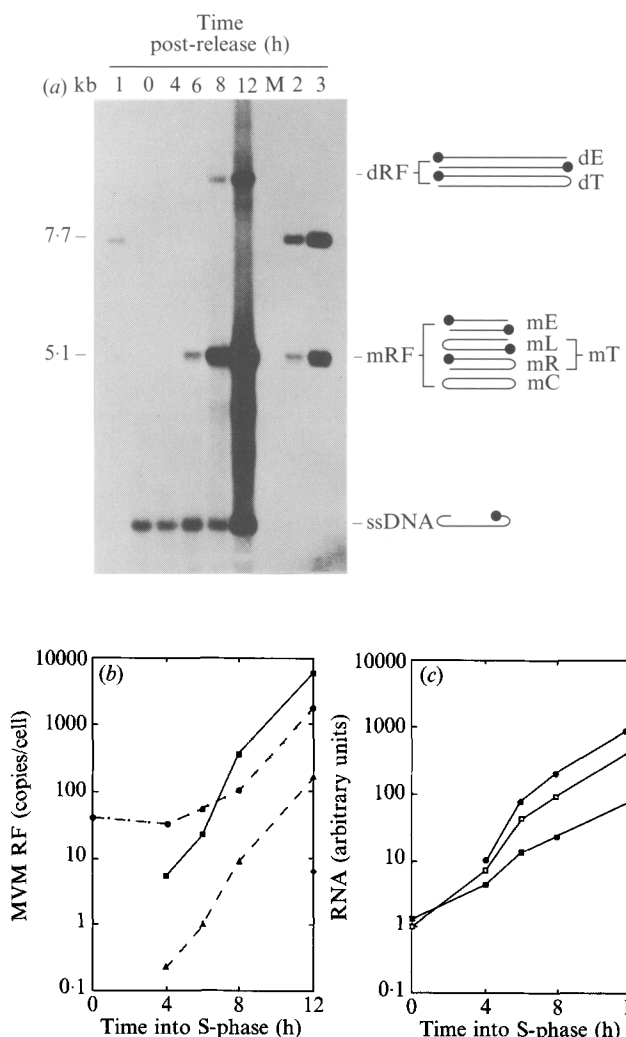


Fig. 1. (a) Southern blot of MVM replicative DNA separated on a 1% agarose gel. At 0, 4, 6, 8 and 12 h after release into the S-phase, cells were rinsed three times with cold PBS and stored at -70°C until lysis. Crude SDS lysates were loaded directly onto agarose gels. This procedure avoids any selective loss of DNA forms that might occur during further extraction. The following number of cell equivalents were loaded in each lane: 0, 4 and 6 h samples (5×10^4), 8 h (2.5×10^4) and 12 h (1×10^4). The position of major MVM RF are indicated. Putative extended and turn-around forms of MVM RF are drawn on the right. Markers were a combination of a full-length MVM clone, pMVM (Tullis *et al.*, 1988), linearized with *Xba*I (7.69 kb) and pMVM digested with *Bam*H I to release the MVM insert (5.15 kb) from the vector (2.54 kb). Three concentrations of markers were used: 0.84 pg (1×10^5 copies of double-stranded MVM; lane 1), 8.40 pg (1×10^6 copies; lane 2) and 42.0 pg (5×10^6 copies; lane 3). Lane M, mock-infected cells. (b) Accumulation of MVM replicative DNA. RF are designated as follows: mRF, ●; dRF, ▲; ssDNA, ■. (c) Accumulation of MVM mRNA during the same synchronized infection shown in Fig. 1(a), 2 and 5, as measured by RNase protection assay as described in Methods. MVM transcripts are designated as follows: R3, ●; R2, □; R1, ■.

measured cell-associated DNA and because MVM progeny virions are preferentially exported from the cell during a highly synchronized infection (Cotmore &

Tattersall, 1989; Tullis *et al.*, 1992), the amount of ssDNA measured here underestimates the total amount produced. In the third experiment, the relative ratio of ssDNA per mRF had not yet begun to increase by 12 h post-release, reflecting the relatively high amount of input ssDNA present in this experiment and a slower accumulation of mRF, probably due to a difference in the infectivity to particle ratios between viral stocks. Presumably, in this experiment the infection had not yet reached the packaging stage.

There is a temporal phasing in the appearance of MVM RNA during infection (Clemens & Pintel, 1988; Schoborg & Pintel, 1991); R1 and R2, which are generated from a promoter at map unit 4, encode the non-structural proteins NS1 and NS2, and are expressed prior to the capsid gene transcripts, R3, generated from a promoter at map unit 38. In the highly synchronous infections described above, the switch from production of predominantly R1 and R2 to predominantly R3 transcripts occurred at about 4 h into the S-phase (Fig. 1c), approximately the same time as DNA replication began (Fig. 1b). By 8 h post-release, R3 had reached its characteristic, steady-state level of approximately 60% of the total MVM RNA. Between 6 and 12 h post-release into the S-phase, both MVM RNA and DNA forms increased exponentially; however, MVM DNA forms accumulated at a faster rate than mRNAs (Fig. 1b and c), suggesting that the number of DNA templates, rather than the production of MVM gene products, is limiting and that the majority of DNA templates were present in a pool of molecules destined for further DNA amplification rather than gene expression.

Analysis of the temporal accumulation of MVM RF in highly synchronous infection by 2D-AGE

Extended and turn-around RF can be effectively separated by 2D-AGE (Cotmore & Tattersall, 1988; Tullis *et al.*, 1993). Under alkaline conditions, mE and viral ssDNA migrate as 5 kb DNA, whereas mT migrate as 10 kb DNA (Fig. 2). Similarly, dRF separates into a 20 kb turn-around dimer (dT) and a 10 kb extended dimer (dE) in the second, alkaline dimension (Fig. 2b and c). In our experiments, a portion of dRF also comigrated with viral 5 kb ssDNA in the alkaline dimension and is probably derived from dRF that are nicked near the middle of the molecule in the dimer bridge region (Fig. 2). This is consistent with previous observations that gel-purified dRF and tetramer RF tend to break down (under neutral conditions) into 5 kb monomeric DNA (Ward & Dadachanji, 1978).

In these experiments, MVM mRF was first detected 3 to 4 h into the S-phase. At this time, 70% of these molecules were extended (mE) (data not shown), sug-

Table 1. Accumulation of MVM RF*

MVM DNA	Experiment	Time post-release (h)									
		0	3	4	5	6	7	8	9	12	
ssDNA† (copies/cell)	1	91.4		104		48.5			320 ± 78	2320 ± 370	
	2	39.2		33.4		47.7		124 ± 32.7		3760 ± 1090	
	3	145	146	94	139	107 ± 16.4	74.5 ± 17.8	124	197 ± 57	1070 ± 120	
mRF (copies/cell)	1	ND‡		ND		15.0			800 ± 290	3290 ± 1130	
	2	ND		< 1		30.2		337		5370 ± 2090	
	3	ND	3.0	2.3	7.4	12.8 ± 6.7	43.3 ± 1.7	78.1	252 ± 14.0	3370	
dRF (copies/cell)	1	ND		ND		1.1 ± 0.90			56.8 ± 7.2	210 ± 22.4	
	2	ND		ND		2.0		26.7 ± 10.1		329 ± 71.4	
	3	ND	ND	ND	< 1	1.2 ± 0.19	4.7 ± 2.1	5.7 ± 1.6	24.2 ± 3.8	252 ± 26.6	
dRF per mRF	1					0.075 ± 0.06			0.071 ± 0.009	0.064 ± 0.007	
	2					0.067		0.079 ± 0.030		0.061 ± 0.013	
	3					0.091 ± 0.015	0.109 ± 0.049	0.073 ± 0.020	0.096 ± 0.015	0.075 ± 0.008	
ss per mRF	1								0.40 ± 0.10	0.71 ± 0.11	
	2								0.37 ± 0.10	0.70 ± 0.20	
	3								1.59	0.78 ± 0.73	
										0.32 ± 0.04	

* 95% confidence limits are given when three or more measurements were averaged.

† Viral ssDNA includes both input and progeny single-stranded DNA and is reported as copies/cell following infection at m.o.i. 0.2.

‡ ND, Not detected (≤ 1 copy of mRF per cell).

gesting that if the incoming ssDNA is first converted to a turn-around form (Fig. 4c, ix), then at least 70% of the mRF present had already been processed at 4 h post-release, either by direct conversion of the left-hand turn-around end to an extended end or through an undetected dRF intermediate. Between 4 and 12 h after release of infected cells into the S-phase, during which time MVM RF is being amplified exponentially, approximately 65% of mRF were mE (Fig. 2; Table 1). By 24 h after release, turn-around forms became more abundant (data not shown), as has been previously reported (Cotmore *et al.*, 1989). A small amount of mC, apparently slightly larger than 10 kb when resolved in the second dimension (Cotmore *et al.*, 1989), was first detected 12 h post-release and accounted for approximately 1% of mRF at that time (Fig. 2c).

Approximately 90% of dRF were dE between 6 and 12 h post-release (Fig. 2). The ratio of extended and turn-around dRF, which have right-hand palindromes on both ends, is similar to the ratio of extended and turn-around right-hand palindromes present in the total replicating pool, as discussed further below. A low level of tetramer RF (approximately six copies/cell) was also visible at 12 h post-release. The majority of tetramer RF migrated as 15 kb DNA fragments in the alkaline dimension, suggesting that, similar to dRF, they were nicked in a left-hand palindrome, approximately 5 kb from one end.

An additional MVM DNA form, termed band X, migrated between ssDNA and mRF in a neutral agarose gel but comigrated with viral ssDNA in the alkaline dimension (Fig. 2). A DNA form similar to band X has been observed previously in crude cell lysates (Cotmore

& Tattersall, 1988) and nuclear extracts (Doerig *et al.*, 1986). A similar DNA form has also been reported to be associated with viral capsids (Doerig *et al.*, 1986; Faust *et al.*, 1989). The DNA component of band X is covalently attached to NS1, similar to MVM RF and progeny ssDNA, because its mobility in SDS-agarose gels is slightly increased following proteinase K treatment and it can be immunoprecipitated with anti-NS1 antibody, even after boiling in 0.2% SDS (Cotmore & Tattersall, 1988; G. Tullis & D. J. Pintel, unpublished results). Band X is also sensitive to mung bean nuclease (Cotmore & Tattersall, 1988; G. Tullis & D. J. Pintel, unpublished results), indicating that at least a portion of the molecule remains single-stranded.

Band X is an RNA-DNA duplex

The alkali sensitivity of band X suggested that it might contain an RNA component. Indeed, band X was susceptible to both RNase A and RNase H (Fig. 3a), indicating that it is a duplex of RNA and DNA. Hybridization of Southern blots of two-dimensional agarose gels with strand-specific RNA probes confirmed that the DNA component of band X is composed primarily of the viral strand (data not shown). The mobility of band X in neutral agarose gels compared with that of ssDNA suggests that the RNA component is at least several kilobases long.

To determine whether this RNA-DNA duplex could form during the lysis procedure, we performed a reconstruction experiment in which 32 P-labelled viral ssDNA was added to MVM-infected cells at the time of lysis. Although an approximately equimolar amount of

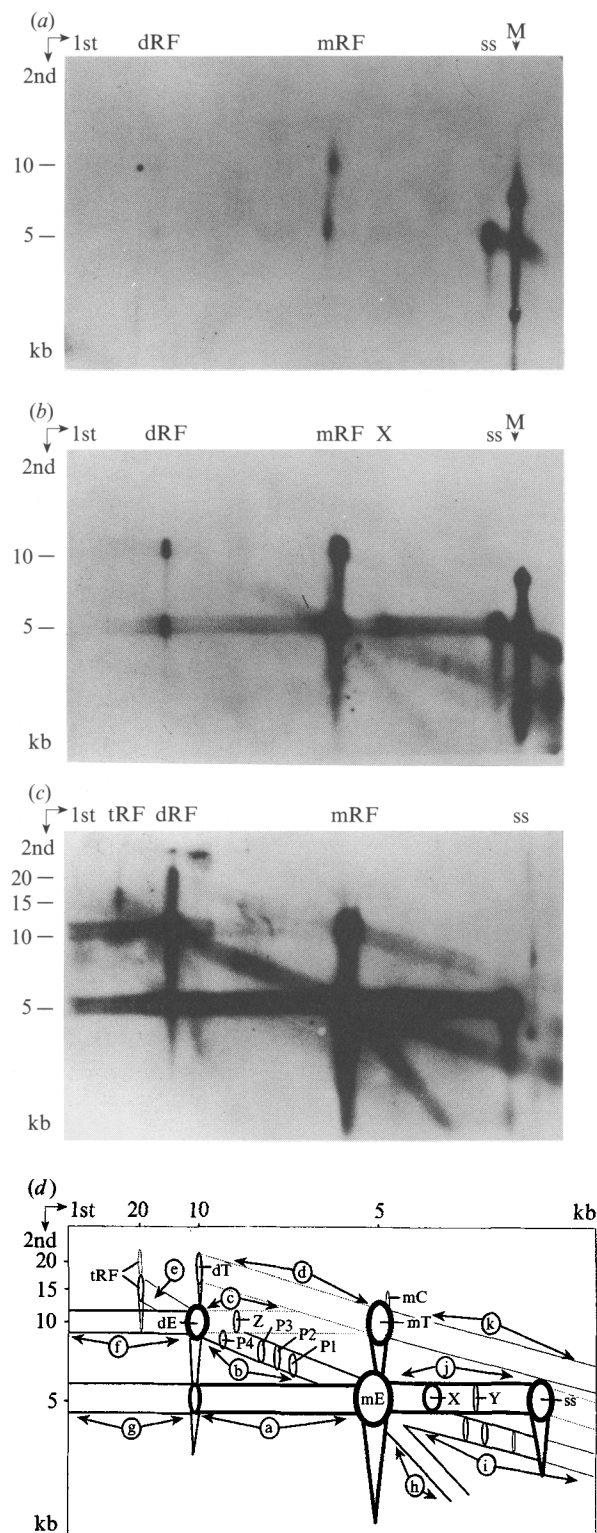


Fig. 2. 2D-AGE analysis of MVM replicative DNA present at (a) 6 h, (b) 8 h and (c) 12 h after release into the S-phase. Lanes containing duplicate samples from the same experiment shown in Fig. 1 were cut out and subjected to electrophoresis through an alkaline agarose gel (30 mM-NaOH, 1 mM-EDTA). (d) Tracing of autoradiograph shown in (c). MVM RF are designated as in the text. Additionally labelled are: viral ssDNA, ss; band X; and two uncharacterized forms Y and Z.

³²P-labelled ssDNA was added to the cells, only a small amount was converted to band X (approximately 6%). The majority of band X present (> 90%) was formed with unlabelled ssDNA (as detected by Southern blot), suggesting that most of band X was formed intracellularly, prior to lysis with SDS (data not shown).

Because band X appeared as early as 4 h into the S-phase, a time at which very little, if any, ssDNA is produced, it seemed likely that band X could also be formed from the incoming viral ssDNA. To address this question, we infected synchronized A9_{2L} cells with ³²P-labelled virus (isolated from infected A9_{2L} cells labelled with [³²P]orthophosphate, 0.24 mCi/ml in medium containing one-tenth the normal amount of phosphate). A mock extract was also prepared from uninfected cells that were labelled with an equivalent amount of [³²P]orthophosphate. ³²P-labelled band X, as well as a low level of mRF, were generated in cells infected with ³²P-labelled virus at 5 h after release of the aphidicolin block (Fig. 3b). Neither MVM form was present in cells incubated with either ³²P-labelled mock lysate, or this labelled lysate to which an equivalent amount of unlabelled virus was added. Therefore, as expected, band X can form from the incoming parental ssDNA. Interestingly, assuming that both mRF and band X are formed from a single input molecule, band X was two- to threefold more abundant at this time.

The biological significance of band X is unclear. An RNA-DNA duplex could be formed by extension from the 3' hydroxyl group of ssDNA by an RNA polymerase, similar to the initial conversion of ssDNA to mRF by a DNA polymerase, such that the RNA component would be covalently joined to the 3' hairpin. However, whereas analogous turn-around forms of parvovirus RF DNA are resistant to heat denaturation (100 °C for 3 min) and quick cooling at 4 °C, because they quickly reanneal, band X was susceptible to this treatment (Fig. 3a, right panel), suggesting that the RNA was not covalently attached. It is unlikely that band X results from non-specific transcription of ssDNA, because X would then be expected to be a much more heterogeneous band than that observed. Since initiation from a ssDNA promoter would be novel for a eukaryotic system, it is also unlikely that band X results from specific transcription of the viral genome. However, the 3'-terminal hairpin could be extended a short distance to create a double-stranded promoter, which could be recognized by RNA polymerase II transcription factors. Further experiments are required to determine whether the RNA component of

DNA that is derived from replicative intermediates is labelled a to k; four putative products of replication pausing are designated P1, P2, P3 and P4, and are discussed in the text.

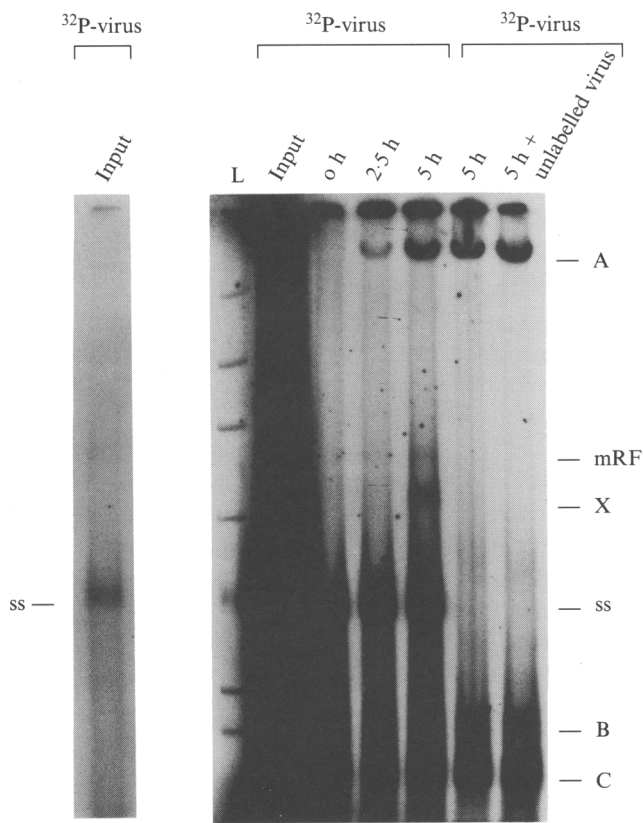
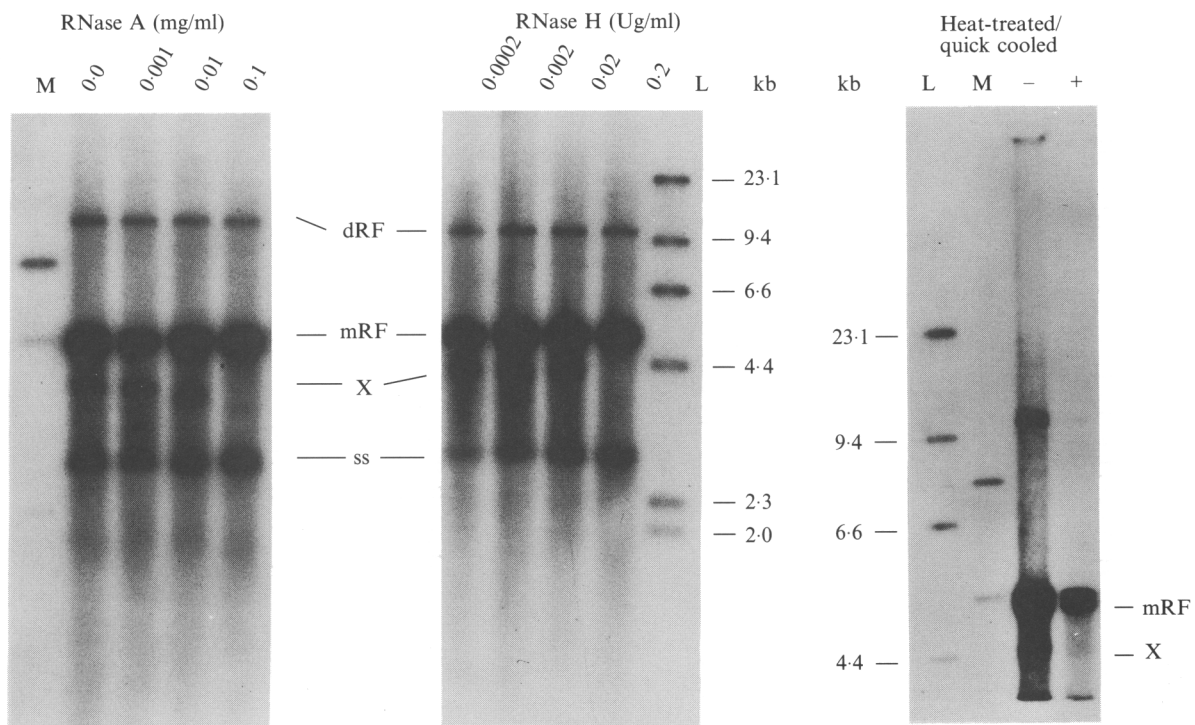


Fig. 3. Band X is an RNA-DNA duplex. (a) Highly synchronous MVM-infected cells were lysed 24 h after release into the S-phase and extracted with phenol-chloroform and precipitated in ethanol. Samples were resuspended without SDS and digested with various amounts of RNase A (left panel) or RNase H (centre panel) at 37 °C for 1 h. MVM-specific DNA forms were analysed by Southern blotting. Infected cell lysates were also analysed by Southern blotting either directly (−) or following denaturation at 100 °C for 3 min and quick cooling to 4 °C (+) (right panel). For all three panels size markers of 7.7 kb and 5.1 kb were derived from a full-length clone of MVM (M); lanes L, end-labelled λ HindIII fragments. (b) Synchronized A9_{2L} cells were infected with ³²P-labelled MVM and lysed at 0, 2.5 and 5 h after release into S-phase. DNA forms were separated in a vertical agarose (1%) gel. An aliquot of the ³²P-labelled virus was also lysed (Input). The panel on the left is a light exposure of the input lane on the right panel. As a control, synchronized A9_{2L} cells were also infected with a mock input prepared from ³²P-labelled uninfected cells. Cells infected with either the mock input alone, or with an equivalent amount of unlabelled virus added, were collected at 5 h after release into the S-phase and lysed. MVM DNA forms are designated as in Fig. 1 and 2. Label from the input was also incorporated into high M_r cellular DNA (A) and two lower M_r species that may correspond to ribosomal RNAs (B and C).

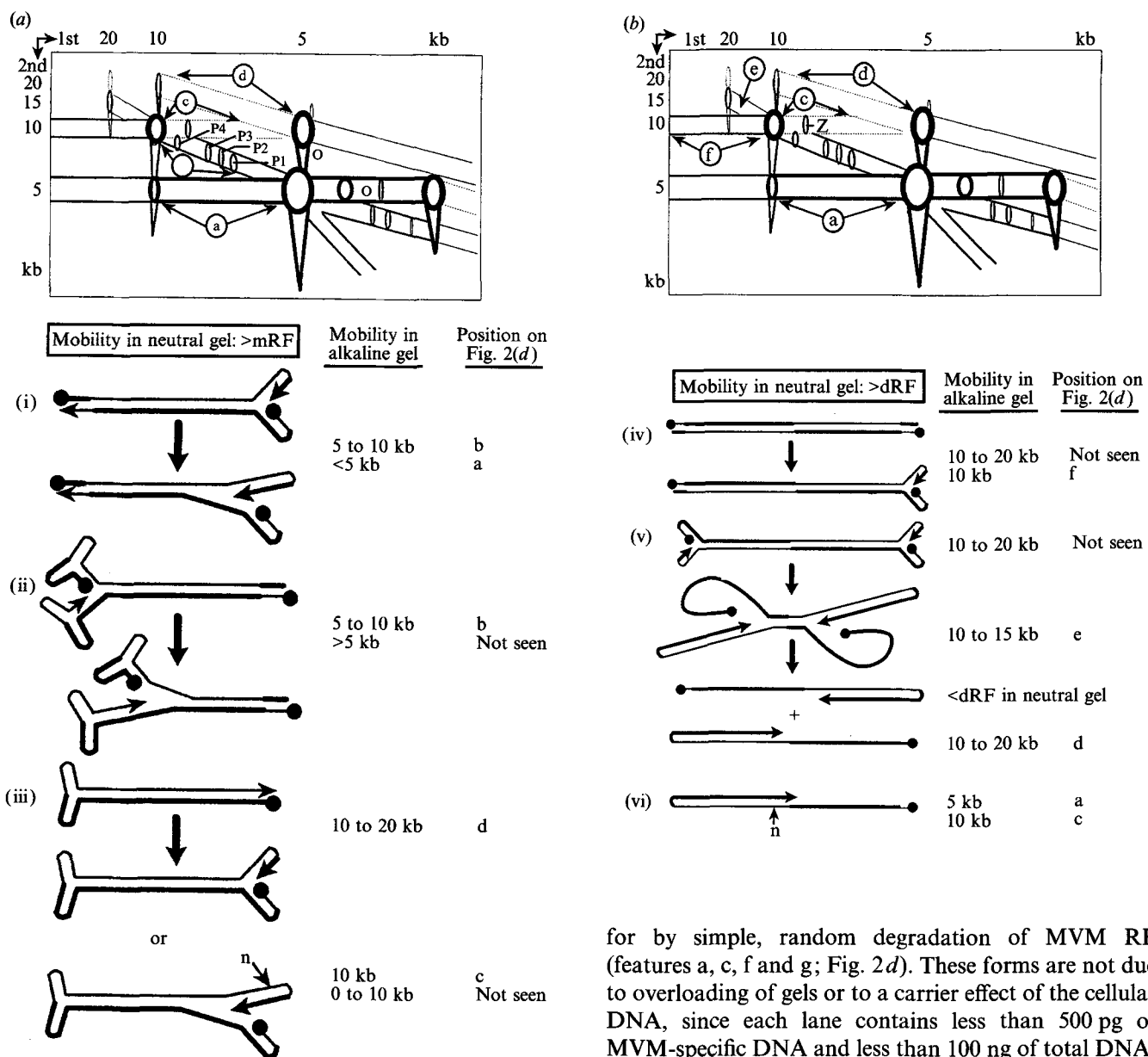


Fig. 4(a) (b). For legend see facing page.

band X is a specific MVM transcript and if it can be formed in the absence of DNA elongation.

Analysis of additional replicative intermediates

In addition to the major viral RF described above, intracellular MVM DNA was separated by 2D-AGE into a reproducible and characteristic pattern of intermediate-sized DNA that progressed throughout infection (Fig. 2). Although random double-stranded breaks may contribute to the DNA seen in some features (e.g. Fig. 2d; b, d, e, i and k), others cannot be accounted

for by simple, random degradation of MVM RF (features a, c, f and g; Fig. 2d). These forms are not due to overloading of gels or to a carrier effect of the cellular DNA, since each lane contains less than 500 pg of MVM-specific DNA and less than 100 ng of total DNA, nor do they correlate with the amount of cell lysate loaded (note that the sample in Fig. 2c contains only one-fifth the number of cell equivalents as the sample shown in Fig. 2a). The 5 kb DNA in a and g of Fig. 2(d) does not derive from aberrant migration of standard 5 kb mRF, because no complementary (plus) strands were detected when blots similar to the one shown in Fig. 2(c) were hybridized to strand-specific RNA probes (data not shown). It is also unlikely that these forms are derived from a protein-induced shift in mobility of viral ssDNA, because infected cells were lysed in 2% SDS, and treatment with proteinase K (0.5 mg/ml at 37 °C for 4 h) prior to electrophoresis did not affect the mobility of this DNA (data not shown). These forms are also not likely to include RNA-DNA hybrids, like band X, because they would have to contain greater than unit

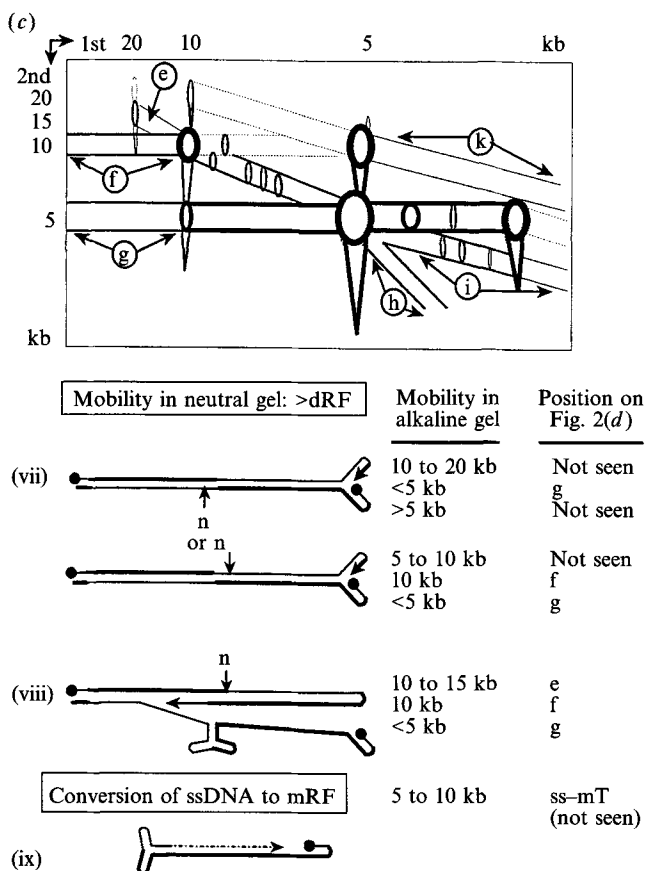


Fig. 4. Potential intermediates in parvoviral replication and their expected mobility in neutral and alkaline agarose gels. (a) Replication of mRF, (b) replication of dRF and (c) replication of nicked dRF and the conversion of ssDNA to mRF. Minus or viral strands are denoted by thick lines. Plus or complementary strands are denoted by thin lines. NS1 is designated by a solid circle. Arrowheads mark 3' ends. Nick sites are designated with an 'n' and an arrow. A drawing of Fig. 2(c) is shown at the top of each with the corresponding DNA intermediates marked.

length RNA and because they were resistant to RNase A (data not shown).

We presume that these viral DNAs are replicative intermediates because the appearance of this DNA parallels the appearance and accumulation of MVM double-stranded RF and not input viral ssDNA. Although we cannot conclusively identify each band, in this section we correlate the presence of these DNA forms with the expected mobility of replicative intermediates predicted to be generated from the replication of a 5 kb, linear double-stranded DNA molecule by a hairpin transfer mechanism.

(i) *Intermediates that migrate between mRF and dRF in the neutral dimension (Fig. 4a; a, b, c, d).* mE that have initiated replication in one end would migrate slower than mRF in a neutral agarose gel (Fig. 4a, structures i and ii), and under alkaline conditions such molecules

would dissociate into a 5 kb strand and an intermediate-sized strand between 5 and 10 kb. Bands consistent with the migration of such forms appear in our analysis as a and b in Fig. 4(a). If initiation occurred at the right end of the genome, the 5 kb non-replicating strand would be the minus strand (Fig. 4a, i); initiation at the left end would generate 5 kb plus strands (Fig. 4a, ii). Alternatively, if DNA replication initiated at both ends of the genome, two intermediate-sized strands would be produced (not depicted in Fig. 4). Hybridization of strand-specific RNA probes to Southern blots similar to the one shown in Fig. 2(c) indicates that 5 kb strands dissociated from replicative intermediates, like the majority of packaged viral DNA, were minus strands (data not shown), suggesting that at 12 h post-release, MVM DNA replication primarily initiates from the right end of the molecule as predicted by current replication models. This result, however, does not formally exclude the possibility that DNA replication initiates on either the left end or both ends on some MVM mRF.

Four areas of increased intensity are seen on diagonal b of Fig. 4(a), designated P1 to P4, which presumably correspond to common pause sites during replication. Based on their relative mobilities in the alkaline dimension and assuming that replication initiates in the right end, we estimate that these putative pause sites roughly map to nucleotides 2900 (P1), 2500 (P2), 2100 (P3) and 900 (P4). P2 and P3 migrate at approximately 7.7 and 8.3 kb respectively in the neutral dimension, similar to the position of the 8 kb intermediate previously described by Faust & Gloor (1984). The mobility of these bands in the alkaline dimension, however, is not consistent with the dimeric intermediate proposed by these authors, which is the same as structure vi in Fig. 4(b). As discussed below, another band, Z, may be derived from such intermediates.

Replicative intermediates generated from mT would migrate between 10 and 20 kb in the alkaline dimension (Fig. 4a, iii). Bands consistent with the migration of such forms appear in our analysis as region d in Fig. 4(a). The end product of such intermediates would be dRF that are covalently closed in the end in which replication originated. The 10 kb DNA strands corresponding to c in Fig. 4(a) could potentially be derived from replicating mT molecules that are nicked in the right-hand palindrome (Fig. 4a, iii), however this is unlikely since such intermediates would also generate 0 to 10 kb replicating strands, which were not detected (Fig. 2c). A more likely alternative is that such 10 kb strands derive from replication intermediates of dRF, as discussed below.

(ii) *Intermediates of dRF replication (Fig. 4b, a, c, d, Z; Fig. 4c, e, f, g).* As with mRF, replication from one end of dE would produce replicating strands between 10 and 20 kb long (Fig. 4b, iv); however, only bands

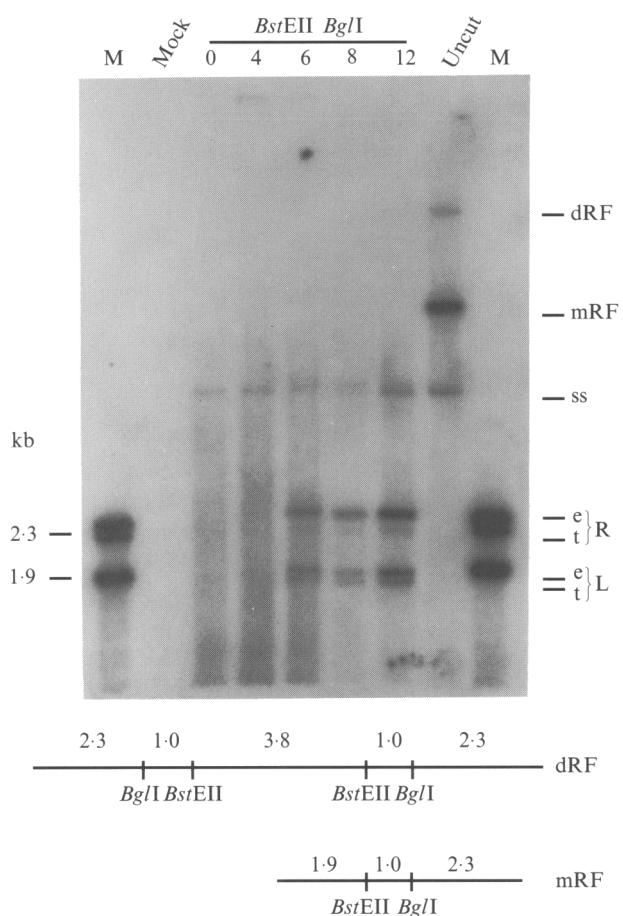


Fig. 5. Southern blot of MVM replicative DNA digested with *Bst*EII and *Bgl*I and separated on a 1.4% agarose gel. *Bst*EII cuts at MVM nt 1886 and *Bgl*I cuts at nt 2872. A map of mRF and dRF showing these restriction sites is shown. mRF is cleaved twice yielding 1.9 kb left-end fragments (nt 1 to 1886), an internal 1.0 kb fragment (nt 1886 to 2872) and 2.3 kb right-end fragments (nt 2872 to 5149). dRF is cleaved four times to yield 2.3 kb right-end terminal fragments, two internal 1.0 kb fragments, and a 3.8 kb bridge fragment across the joined left-hand ends. Left (L; 1.9 kb) and right (R; 2.3 kb) turn-around (t) or extended (e) end fragments are designated. Samples were from the same experiment as shown in Fig. 1 and 2. Markers were pMVM digested with *Bam*H I, *Bst*EII and *Bgl*I to give fragments of 2.3, 1.9, 1.2, 1.0, 0.9 and 0.4 kb. Because this gel was run to maximize the separation of left and right end extended and turn-around fragments, the 1.0 kb fragments have run off; also, in this particular gel, the 3.8 kb dimer bridge fragments comigrate with single strand. An additional band at 2.2 kb is also seen due to a small deletion in the right-hand end of MVM, which occurs spontaneously in *Escherichia coli* (Merchlinsky, 1984; Astell *et al.*, 1985).

consistent with the migration of intermediates ranging between 10 and 15 kb were detected (Fig. 4*b*, *e*). Because dRF, unlike mRF, contain potential replication origins on both ends of the molecule, replicating strands might be limited to 15 kb because the two strands would dissociate as the replication forks approach the middle of the molecule (Fig. 4*b*, *v*). Once dissociated, these intermediates would migrate faster than dRF in the

neutral dimension, and between 10 and 20 kb in the alkaline dimension, corresponding to the upper half of diagonal *d* in Fig. 4(*b*). Because dRF are specifically nicked in the dimer bridge, dimer intermediates might be predicted to also be nicked; however, the replication of dimer molecules that have been previously nicked in either the template or opposite strand would generate 5 to 10 kb or 5 kb plus strands, respectively (neither of which is detected) and not 10 to 15 kb DNA (Fig. 4*c*, *vii*). Alternatively, replicating strands between 10 and 15 kb could also be generated if the template strand were nicked after the replication fork has passed through the dimer bridge (Fig. 4*c*, *viii*). This model is plausible because the terminal protein, NS1, is also responsible for the nicking of the dimer bridge (Cotmore & Tattersall, 1992; Cotmore *et al.*, 1992, 1993). If terminal NS1 remains associated with the replication complex, then it could potentially nick the dimer bridge as the replication fork passes through its recognition sequence, similar to the activity of the gene A protein in the termination of ϕ X174 DNA replication (Eisenberg *et al.*, 1977; Reinberg *et al.*, 1983). Replication intermediates of dRF that initiated from both ends might be similarly nicked following replication of the left-hand palindrome (Fig. 4*b*, *vi*) to generate two 5 kb minus strands (Fig. 4*b*, *a*) and two strands of approximately 10 kb (Fig. 4*b*, *c*) under denaturing conditions. In our analysis 5 and 10 kb strands (Fig. 4*b*, *a* and *c*) appear concentrated in an area that migrates at approximately 9 kb in the neutral dimension (designated *Z* in Fig. 4*b*) and so may be derived from such an intermediate which may be identical to the 8 kb metastable, dimeric intermediate proposed by Faust & Gloor (1984). As also reported for dRF (Ward & Dadachanji, 1978), this intermediate tended to break down into 5 kb ssDNA and mRF, suggesting that it might also be nicked in the dimer bridge (Faust & Gloor, 1984).

(iii) *Intermediates that migrate faster than mRF in the neutral dimension (Fig. 4*c*; *h*, *i*, *j*, *k*).* Conversion of ssDNA to mRF by extension from the 3'-terminal palindrome should generate replicative intermediates that migrate between ssDNA and mT in both the neutral and alkaline dimensions (Fig. 4*c*, *ix*). Bands consistent with the migration of such DNA intermediates, however, were not detected (Fig. 2). Diagonal *k*, present at 12 h post-release, does not intersect ssDNA, but rather passes just above (Fig. 4*c*, *k*), and therefore is not derived from ssDNA. The migration of *k* is consistent with that of a double-stranded turn-around form. [For example, in the 2D-AGE shown in Fig. 2, a 3 kb molecule that is covalently closed in one end would approximately comigrate with ssDNA in the neutral dimension, but migrate above ssDNA in the alkaline dimension (at 6 kb).] Such forms present in our analysis may be turn-

Table 2. Accumulation of extended and turn-around forms*

Proportion of RF (%)	Experiment	Time post-release (h)						
		3	4	5	6	7	8	9
mT†	1				32.0			31.8 ± 15.9
	2				44.6			38.7 ± 6.61
	3	24.9	29.4	32.9 ± 7.70	28.5	37.0 ± 5.80	29.1 ± 9.48	28.6 ± 4.05
L _t ‡	1				36.9			30.8
	2				36.2		32.0 ± 6.14	42.3 ± 7.83
	3					34.6 ± 10.75	29.3 ± 8.01	31.2 ± 2.82
R _t §	1				ND			30.8 ± 4.97
	2				20.3		13.5 ± 3.17	10.2 ± 5.20
	3					ND	10.6 ± 5.52	11.6 ± 3.66

* 95% confidence limits are given when three or more measurements were averaged.

† mT is calculated as the percentage of total monomeric replicative forms that migrate at 10 kb in the alkaline dimension or were resistant to heat denaturation and quick cooling [%mT = mT (100)/(mE + mT + mC)].

‡ L_t is the proportion of left end restriction fragments that were resistant to heat denaturation and quick cooling [%L_t = L_t (100)/(L_t + L_e)].

§ R_t is the proportion of right end restriction fragments that were resistant to heat denaturation and quick cooling [%R_t = R_t (100)/(R_t + R_e)].

|| ND, Not detected.

around forms of defective RF or derive from random double-stranded breaks in mT. Corresponding extended forms of defective RF would migrate on the diagonal between 0 and 5 kb (Fig. 4*c, i*). (The identity of diagonal h, which also migrates between 0 and 5 kb in the alkaline dimension but correspondingly slower in the neutral dimension, is unknown.)

The absence of replicative intermediates between ssDNA and mT suggests that the conversion of ssDNA to mRF is not an active pathway for replication at 8 and 12 h post-release, although such intermediates may be present at levels below our limit of detection. This result is consistent with previous observations that most, if not all, of the progeny ssDNA produced is concurrently packaged (Cotmore & Tattersall, 1987), and argues against a model in which MVM produces significant amounts of both plus and minus strands, selectively packages the minus strands and recycles plus strands to mT. Alternatively, intermediates between ssDNA and mRF also might remain undetected if the left hairpin was nicked (or open-ended), since such molecules would generate a 5 kb band and an intermediate-length strand (0 to 5 kb) corresponding to sections *a* and *i* on Fig. 2(*d*). However, this alternative seems unlikely because data presented below indicate that neither left nor right turn-around ends were nicked in the terminal hairpin.

Quantification of extended and turn-around left- and right-hand ends

2D-AGE allows a direct quantification of the relative amounts of extended and turn-around forms of mRF and dRF (Table 1); however, this technique does not distinguish between mL and mR. Left and right covalently closed ends can be distinguished from their

extended counterparts by 1D-AGE following restriction enzyme digestion (Fig. 5). The identities of these turn-around end fragments were confirmed by both 2D-AGE and their resistance to heat denaturation (100 °C for 3 min) and quick cooling (at 4 °C) (data not shown).

Because dRF do not contribute to 1.9 kb left end fragments (Fig. 5, bottom), the ratio of turn-around and extended left end fragments (L_t and L_e, respectively) should reflect the ratio of mRF that are covalently closed in the left end, that is L_t = mL + mC and L_e = mE + mR. During the time course presented here, 30 to 40% of left end fragments were covalently closed (Table 2). This was approximately the same percentage as found for total mT, suggesting that little or no mRF are turn-around in the right end. However, approximately 10% of right end fragments were also found to be turn-around by restriction digestion analysis (Fig. 5, Table 2). Although dRF contributes to the pool of 2.3 kb right end fragments, it is unlikely that all of the turn-around right end fragments observed are derived from dRF, because essentially all dRF would have to be turn-around in both ends in order to account for the amount of turn-around right-end fragments detected. On the contrary, our 2D-AGE analysis suggested that greater than 90% of dRF were extended on both ends. It is also unlikely that the amount of mT was underestimated owing to specific nicks in the termini because > 90% of turn-around end fragments were resistant to heat denaturation and quick cooling (data not shown). Quantification of left- and right-hand ends by 1D- and 2D-AGE following *Bst*EII and *Bgl*I restriction digestion further confirmed that > 85% of turn-around right end fragments and > 95% of left end turn-around fragments were intact (data not shown).

A more likely possibility that would account for the

Table 3. Extended and turn-around forms of monomer

Proportion of mRF (%)	Experiment	Time post-release (h)				
		6	7	8	9	12
mE	1	65.6			65.9	57.1
	2	52.5		67.2		68.9
	3		63.4	66.1	65.7	67.1
mL	Average	59.1		66.7	65.8	64.4
	1	34.4			28.7	37.0
	2	32.2		25.5		24.6
mR	3		35.4	26.7	29.1	26.8
	Average	33.3		26.1	28.9	29.5
	1	< 1			5.4	5.9
	2	15.3		7.3		6.5
	3		1.1	7.3	5.3	6.2
	Average	7.7		7.3	5.4	6.2

increase in turn-around ends detected following restriction enzyme digestion is that partially replicated intermediates contribute to the number of turn-around end fragments observed (Fig. 5). Two observations suggest that this might be the case: (i) restriction enzyme digestion reduces the average size of the background of replicative intermediates in one-dimensional agarose gels and (ii) at 12 h post-release the sum of right, left and middle fragments produced by restriction enzyme digestion was greater than the sum of mRF and dRF (Fig. 5; G. Tullis & D. J. Pintel, unpublished results). These replicative intermediates apparently contribute a higher proportion of turn-around ends relative to extended ends, such that $mL \leq L_t$ and $mR \leq R_t$. A lower limit for mL and mR, however, can be estimated from measurements of R_t and L_t , respectively ($mL \geq mT - R_t$ and $mR \geq mT - L_t$). Based on these calculations, approximately 30% of the total mRF are covalently closed in the left end and less than 10% are covalently closed in the right end (Table 3).

If mR are formed from initiation of DNA replication in the right-hand hairpin, how are mL formed? Current models of MVM replication rely on the conversion of progeny ssDNA to generate mL. Our results, however, suggest that this point may need to be re-examined. 2D-AGE analysis of MVM DNA did not reveal a significant amount of DNA forms with the mobility expected for intermediates between ssDNA and mL at either 8 or 12 h after release of cells into the S-phase. Either such intermediates are present at a level below our detection limit, or DNA replication may initiate directly in the left-hand palindrome of mE, such that mE is processed to generate mL and mR. Conceivably, mL could also be formed following replication of the plus strand from the right hairpin to form an mC molecule rather than mR, which would then be converted to mL by a strand transfer step by NS1. This pathway seems unlikely because mC were not detected at appreciable levels until

12 h after release of infected cells into the S-phase (Fig. 2).

If mL is produced from progeny ssDNA or directly from mE, the initiation of packaging should lead to a selective amplification of mE over mL. Since progeny ssDNA has been observed to have been packaged as early as 6 h post-release (Cotmore & Tattersall, 1987), this pathway might account for the surplus of mE observed (65% of the total mRF). The ratio of mE relative to mL however remained approximately 2:1 throughout the time-course of these experiments, and no increase in mL was detected at 12 h post-release when an increase in ssDNA was observed. In addition, at much later times (24 to 48 h post-release) turn-around forms and not mE become predominant (data not shown) (Cotmore *et al.*, 1989).

Based on their observation that capsids bind specifically to the left hairpin and not the extended form, Willwand & Kaaden (1990) have proposed a model for the replication of Aleutian disease virus (ADV) in which mL may also be a precursor to packaged ssDNA. According to this model, one mL will produce one mC plus one ssDNA during the packaging phase. mC molecules can then be converted back to mL by NS1, leading to an amplification of this form instead of mE. Since MVM capsids also bind to the left hairpin (Willwand & Hirt, 1991), a similar model could be invoked for MVM replication. However, capsid-deficient MVM mutants, which replicate RF but not ssDNA following transfection into A9_{2L} cells, do not produce a disproportionate amount of either mL or mE in mutant RF compared to wild-type MVM DNA (Tullis *et al.*, 1993). These mutants also accumulate mT in a fashion similar to that observed with wild-type MVM at later times (Tullis *et al.*, 1993). It is not clear, therefore, whether the accumulation of mT reflects a change in the replication pattern, such as entering a packaging phase, or is merely a consequence of the infection. For example, as the cells are killed during infection, open-ended forms may be more susceptible to endonucleases. [Turn-around forms are resistant to endonucleases *in vitro* (Cotmore *et al.*, 1989).]

The kinetic hairpin transfer model, as developed thus far, does not adequately account for the accumulation of mL in MVM DNA replication. Another source of mL may be in the resolution of dRF. The modified rolling hairpin model of Astell *et al.* (1983, 1985) proposes that NS1 may convert dRF to two mRF molecules (one mE and one mL) by a nicking and strand transfer mechanism (Astell *et al.*, 1983, 1985). Experimental evidence also suggests that dRF may be resolved by such a mechanism; plasmids that contain the MVM dimer bridge are resolved into both extended and turn-around ends following transfection into murine cells superinfected

with MVM or with recombinant vaccinia virus that expresses NS1 (Cotmore & Tattersall, 1992; Cotmore *et al.*, 1993), although dRF may be resolved into two mL molecules, one of which is converted into mE. Our 2D-AGE analysis of MVM DNA also indicates that a significant proportion of dRF and higher concatemers are nicked in the left-hand palindrome, suggesting that resolution of dRF into two mLs may occur via single-stranded nicks rather than a double-stranded cut. These results do not address the basic premise of the kinetic hairpin model (i.e. that only the flop orientation of the left hairpin can be processed by a hairpin transfer mechanism), but do suggest that this model should be adjusted to include a strand transfer or similar mechanism, for the resolution of dRF, in order to account adequately for the production of mL. The resolution of dRF, however, does not necessarily require the same strand specificity as originally invoked by Astell *et al.* (1983, 1985).

We thank Lisa Burger for excellent technical assistance and Nathalie Salome for critical reading of the manuscript. R.V.S. was partially supported by the University of Missouri Molecular Biology Program during a portion of this work. This work was supported by PHS grants RO1 AI21302 and KO4 AI00934 from the NIH to D.J.P.

References

- ASTELL, C. R., THOMSON, M., CHOW, M. D. & WARD, D. C. (1983). Structure and replication of minute virus of mice DNA. *Cold Spring Harbor Symposia on Quantitative Biology* **47**, 751–762.
- ASTELL, C. R., CHOW, M. D. & WARD, D. C. (1985). Sequence analysis of the termini of virion and replicative forms of minute virus of mice DNA suggests a modified rolling hairpin model for autonomous parvovirus DNA replication. *Journal of Virology* **54**, 171–177.
- BATES, R. C., SNYDER, C. E., BANERJEE, P. T. & MITRA, S. (1984). Autonomous parvovirus LullIII encapsidates equal amounts of plus and minus DNA strands. *Journal of Virology* **49**, 319–324.
- CAVALIER-SMITH, T. (1974). Palindromic base sequences and replication of eukaryotic chromosome ends. *Nature, London* **250**, 467–470.
- CHEN, K. C., TYSON, J. J., LEDERMAN, M., STOUT, E. R. & BATES, R. C. (1989). A kinetic hairpin transfer model for parvoviral DNA replication. *Journal of Molecular Biology* **208**, 283–296.
- CLEMENS, K. E. & PINTEL, D. J. (1988). The two transcription units of the autonomous parvovirus minute virus of mice are transcribed in a temporal order. *Journal of Virology* **62**, 1448–1451.
- COTMORE, S. F. & TATTERSALL, P. (1987). The autonomously replicating parvoviruses of vertebrates. *Advances in Virus Research* **33**, 91–174.
- COTMORE, S. F. & TATTERSALL, P. (1988). The NS-1 polypeptide of minute virus of mice is covalently attached to the 5' termini of duplex replicative-form DNA and progeny single strands. *Journal of Virology* **62**, 851–860.
- COTMORE, S. F. & TATTERSALL, P. (1989). A genome-linked copy of the NS-1 polypeptide is located on the outside of infectious parvovirus particles. *Journal of Virology* **63**, 3902–3911.
- COTMORE, S. F. & TATTERSALL, P. (1992). *In vivo* resolution of circular plasmids containing concatemer junction fragments from minute virus of mice DNA and their subsequent replication as linear molecules. *Journal of Virology* **66**, 420–431.
- COTMORE, S. F., GUNTHER, M. & TATTERSALL, P. (1989). Evidence for a ligation step in the DNA replication of the autonomous parvovirus minute virus of mice. *Journal of Virology* **63**, 1002–1006.
- COTMORE, S. F., NÜESCH, J. P. F. & TATTERSALL, P. (1992). *In vitro* excision and replication of 5' telomeres of minute virus of mice DNA from cloned palindromic concatemer junctions. *Virology* **190**, 365–377.
- COTMORE, S. F., NÜESCH, J. P. F. & TATTERSALL, P. (1993). Asymmetric resolution of a parvovirus palindrome *in vitro*. *Journal of Virology* **67**, 1579–1589.
- DOERIG, C., McMASTER, G., SOGO, J., BRUGGMANN, H. & BEARD, P. (1986). Nucleoprotein complexes of MVM have a distinct structure different from that of chromatin. *Journal of Virology* **58**, 817–824.
- EISENBERG, S., GRIFFITH, J. & KORNBERG, A. (1977). PhiX174 cistron A protein is a multifunctional enzyme in DNA replication. *Proceedings of the National Academy of Sciences, U.S.A.* **74**, 3198–3202.
- FAUST, E. A. & GLOOR, G. (1984). Characterization of a metastable, partially replicated dimeric intermediate of minute virus of mice. *Journal of Virology* **49**, 621–625.
- FAUST, E. A., BRUDZYNSKA, K. & MORGAN, J. (1989). Characterization of novel populations of MVM virions containing covalent DNA-protein complexes. *Virology* **168**, 128–137.
- FEINBERG, A. P. & VOGELSTEIN, B. (1983). A technique for radiolabeling DNA restriction endonuclease fragments to high specific activity. *Analytical Biochemistry* **132**, 6–13.
- HIRT, B. (1967). Selective extraction of polyoma DNA from infected mouse cell cultures. *Journal of Molecular Biology* **26**, 365–369.
- LUSBY, E., BOHENZKY, R. & BERNS, K. I. (1981). Inverted terminal repetitions in adeno-associated virus DNA: independence of the orientation at either end of the genome. *Journal of Virology* **37**, 1083–1086.
- MANIATIS, T., FRITSCH, E. F. & SAMBROOK, J. (1982). *Molecular Cloning: A Laboratory Manual*. New York: Cold Spring Harbor Laboratory.
- MERCHILINSKY, M. J. (1984). *Studies on MVM DNA replication using an infectious molecular clone*. Ph.D. thesis, Yale University.
- MULLER, D.-E. & SIEGL, G. (1983). Maturation of parvovirus LuIII in a subcellular system. I. Optimal conditions for *in vitro* synthesis and encapsidation of viral DNA. *Journal of General Virology* **64**, 1043–1054.
- OGDEN, R. C. & ADAMS, D. A. (1987). Electrophoresis in agarose and acrylamide gels. *Methods in Enzymology* **152**, 61–87.
- REINBERG, D., ZIPURSKY, S. L., WEISBECK, P., BROWN, D. & HURWITZ, J. (1983). Studies on the phiX174 gene A protein-mediated termination of leading strand DNA synthesis. *Journal of Biological Chemistry* **258**, 529–537.
- SCHOBORG, R. V. & PINTEL, D. J. (1991). Accumulation of MVM gene products is differentially regulated by transcription initiation, RNA processing and protein stability. *Virology* **181**, 22–34.
- STRAUS, S. E., SEBRING, E. D. & ROSE, J. A. (1976). Concatemers of alternating plus and minus strands are intermediates in adeno-associated virus DNA synthesis. *Proceedings of the National Academy of Sciences, U.S.A.* **73**, 742–746.
- TATTERSALL, P. & BRATTON, J. (1983). Reciprocal productive and restrictive virus-cell interactions of immunosuppressive and prototype strains of minute virus of mice. *Journal of Virology* **46**, 944–955.
- TATTERSALL, P. & WARD, D. C. (1976). Rolling hairpin model for replication of parvovirus and linear chromosomal DNA. *Nature, London* **263**, 106.
- TULLIS, G. E., LABIENIEC-PINTEL, L., CLEMENS, K. E. & PINTEL, D. (1988). Generation and characterization of a temperature sensitive mutation in the NS-1 gene of the autonomous parvovirus minute virus of mice. *Journal of Virology* **62**, 2736–2744.
- TULLIS, G. E., BURGER, L. R. & PINTEL, D. J. (1992). The trypsin-sensitive RVER domain in the capsid proteins of minute virus of mice is required for efficient cell binding and viral infection but not for proteolytic processing *in vivo*. *Virology* **191**, 846–857.
- TULLIS, G. E., BURGER, L. R. & PINTEL, D. J. (1993). The minor capsid protein VP1 of the autonomous parvovirus minute virus of mice is dispensable for encapsidation of progeny single-stranded DNA but is required for infectivity. *Journal of Virology* **67**, 131–141.
- TYSON, J. J., CHEN, K. C., LEDERMAN, M. & BATES, R. C. (1990). Analysis of the kinetic hairpin transfer model for parvoviral DNA replication. *Journal of Theoretical Biology* **144**, 155–169.
- WARD, D. C. & DADACHANJI, D. K. (1978). Replication of minute virus of mice DNA. In *Replication of Mammalian Parvoviruses*, pp.

297–313. Edited by D. C. Ward & P. J. Tattersall. New York: Cold Spring Harbor Laboratory.

WILLWAND, K. & KAADEN, O. R. (1990). Proteins of viral and cellular origin bind to the Aleutian disease virus (ADV) DNA 3'-terminal hairpin: presentation of a scheme for encapsidation of ADV DNA. *Journal of Virology* **64**, 1598–1605.

WILLWAND, K. & HIRT, B. (1991). The minute virus of mice capsid specifically recognizes the 3' hairpin structure of the viral replicative-form DNA: mapping of the binding site by hydroxyl radical footprinting. *Journal of Virology* **65**, 4629–4635.

(Received 25 October 1993; Accepted 14 January 1994)